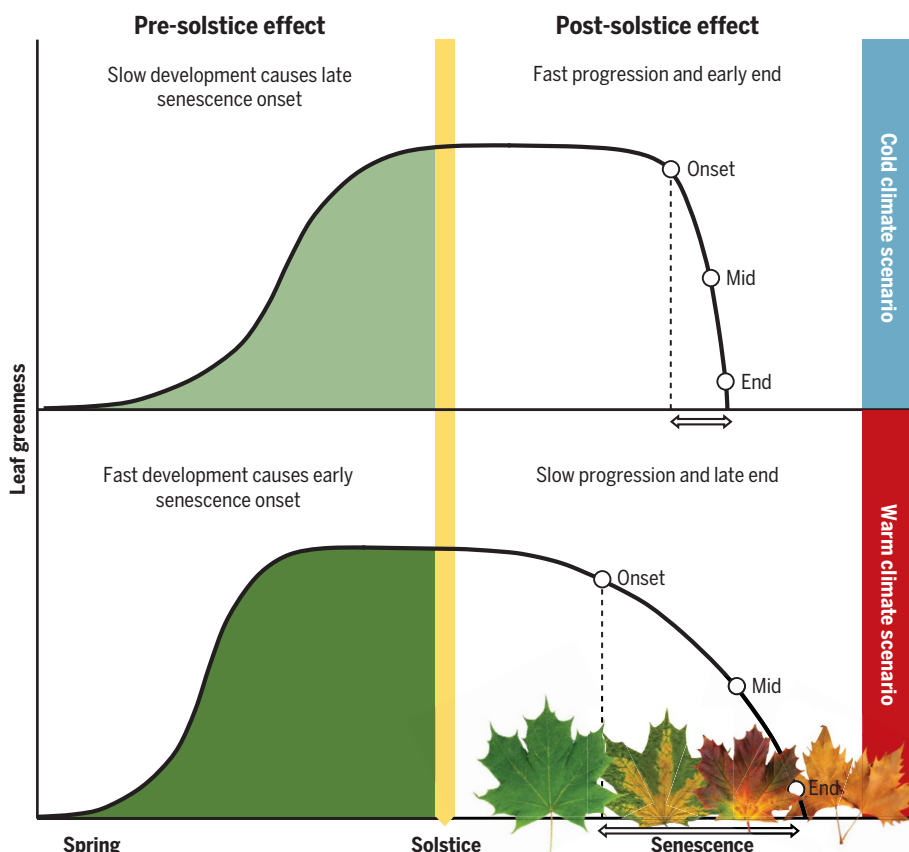# RESEARCH ARTICLE SUMMARY

FOREST PHENOLOGY

Effect of climate warming on the timing of autumn leaf senescence reverses after the summer solstice

Constantin M. Zohner*, Leila Mirzagholi, Susanne S. Renner, Lidong Mo, Dominic Rebindaine, Raymo Bucher, Daniel Palouš, Yann Vitasse, Yongshuo H. Fu, Benjamin D. Stocker, Thomas W. Crowther

INTRODUCTION: Ongoing climate change is causing rapid shifts in plant phenology, with far-reaching effects on the terrestrial carbon cycle and biodiversity. While advances in spring leaf-out dates in temperate and boreal forests are well documented, the effects on autumn leaf senescence are less clear. This is because leaf senescence is not only affected by temperature but also by day length and vegetation activity early in the season in ways that are poorly understood. Accurately predicting future growing-season lengths and plant photosynthesis requires a better understanding of these interacting mechanisms at broad spatial scales.

RATIONALE: Local observations and experiments suggest that early-season warming, causing earlier spring leaf-out and faster plant development, tends to advance autumn senescence dates. Conversely, late-season warming tends to delay autumn senescence. If true more generally, then climate warming has opposing effects at the start and end of the growing season, with a reversal of effects somewhere in between. To test the generality of the opposing effects of climate warming on leaf senescence in Northern Hemisphere forests, we used satellite, ground, and carbon flux data, as well as controlled experiments.

RESULTS: Our results revealed that warming early and late in the growing season indeed has contrasting effects on leaf senescence, with a reversal occurring after the summer solstice. Across 84% of the northern forest area, we found that warmer temperatures and increased vegetation activity before the solstice advance the onset of senescence by 1.9 ± 0.1 days per °C, whereas warmer post-solstice temperatures slow the progression of senescence by 2.6 ± 0.1 days per °C. Between 1966 and 2015, the earlier onset of senescence has led to advances of 0.20 ± 0.07 days per year of the date at which autumn temperature starts to drive senescence progression. By contrast, mid-senescence continues to occur slightly later by 0.04 ± 0.01 days per year, leading to a lengthening of the autumnal senescence period.

In our experiments, warmer pre-solstice temperatures also led to earlier primary growth cessation (bud set), demonstrating that the impact of a warmer pre-solstice period extends beyond leaf development and life span. This highlights the crucial role of overall plant development and sink activity before the summer solstice in determining growing-season length.

CONCLUSION: We have developed a unified explanatory framework for predicting autumn phenology, showing that leaf senescence now tends to begin earlier, because of increased pre-solstice vegetation activity, but progresses more slowly, such that the end of senescence occurs later. The reversal in trees' responsiveness to warming after the summer solstice likely is triggered by changes in day length and allows them to initiate the physiological processes of leaf senescence and nutrient resorption in a fine-tuned balance between source and sink dynamics. Our results demonstrate the impact of developmental constraints (from cell and tissue growth) on autumn leaf senescence and forest productivity, affecting trends in growing-season length across the entire Northern Hemisphere. These insights provide a better understanding of the changes in growing seasons and carbon uptake of temperate and boreal forests under climate change. ∎

Autumn phenological responses to pre-solstice and post-solstice climate warming. In cold years, slow development before the summer solstice delays the onset of senescence, and cold autumn temperatures accelerate senescence progression. In warm years, fast development before the summer solstice advances senescence onset, and warm autumn temperatures slow senescence progression, delaying the end of senescence.

READ THE FULL ARTICLE AT
https://doi.org/10.1126/science.adf5098

RESEARCH ARTICLE

FOREST PHENOLOGY

Effect of climate warming on the timing of autumn leaf senescence reverses after the summer solstice

Constantin M. Zohner[1]*, Leila Mirzagholi[1,2], Susanne S. Renner[3], Lidong Mo[1], Dominic Rebindaine[1], Raymo Bucher[1], Daniel Palouš[1,4], Yann Vitasse[5], Yongshuo H. Fu[6], Benjamin D. Stocker[7,8], Thomas W. Crowther[1]

Climate change is shifting the growing seasons of plants, affecting species performance and biogeochemical cycles. Yet how the timing of autumn leaf senescence in Northern Hemisphere forests will change remains uncertain. Using satellite, ground, carbon flux, and experimental data, we show that early-season and late-season warming have opposite effects on leaf senescence, with a reversal occurring after the year's longest day (the summer solstice). Across 84% of the northern forest area, increased temperature and vegetation activity before the solstice led to an earlier senescence onset of, on average, 1.9 ± 0.1 days per °C, whereas warmer post-solstice temperatures extended senescence duration by 2.6 ± 0.1 days per °C. The current trajectories toward an earlier onset and slowed progression of senescence affect Northern Hemisphere–wide trends in growing-season length and forest productivity.

T he phenological cycles of trees exert a strong control on the structure and functioning of ecosystems (*1, 2*) and global carbon, water, and nutrient cycles (*3–5*). Anthropogenic climate change has resulted in shifts in the growing seasons of temperate and boreal trees, with the start of the season today occurring, on average, two weeks earlier than it did during the 19th and 20th centuries (*6*) and the end of the season (EOS) being delayed (*4, 7, 8*). Each day of a longer growing season may increase net ecosystem carbon uptake by 3.0 to 9.8 gC m^{-2} (*4*). Yet, owing to the complex and interacting effects of growing-season climate and the annual day-length cycle, the direction of EOS changes in response to climate change and the cascading effects on ecosystem productivity remain highly uncertain (*9–13*).

Characterizing the interplay among the environmental drivers of EOS at broad spatial scales is integral to improving our understanding of growing-season length and tree growth. Cell division, tissue formation, and growth in northern trees are highest at the beginning of the season and decline with shortening days (*14–18*), the adaptive reason being the limited time remaining for tissue maturation and bud set before the first frost (*19*). Local observations and experiments have shown that early-season warming, causing earlier spring leaf-out and faster growth and tissue maturation, tends to advance EOS dates (*9, 11, 20, 21*), whereas late-season warming has the opposite effect, delaying the EOS (*22–24*). Increased temperatures and physiological activity in the beginning of the season might drive earlier autumn senescence through a variety of possible mechanisms, including developmental and nutrient constraints (*9, 25, 26*), seasonal buildup of water stress (*27, 28*), and radiation-induced leaf aging (*29*). In contrast, later in the season, a direct effect of temperature (cooling) is likely to drive the timing of autumn senescence (*10, 24, 30*). If these trends are correct, then climate warming has opposing effects at the start and end of the growing season, with a reversal of effects somewhere in between.

In this study, we tested whether early-season temperature and vegetation activity drive an earlier EOS across temperate and boreal forests, with day length providing the linkage between seasonal activity, air warming, and autumn phenology (Fig. 1). We expected that early-season plant development and growth determine the onset of senescence (Fig. 1, scenario 1 versus 2), while autumn temperature affects senescence progression (toward full dormancy), with faster chlorophyll breakdown in colder autumns than in warmer
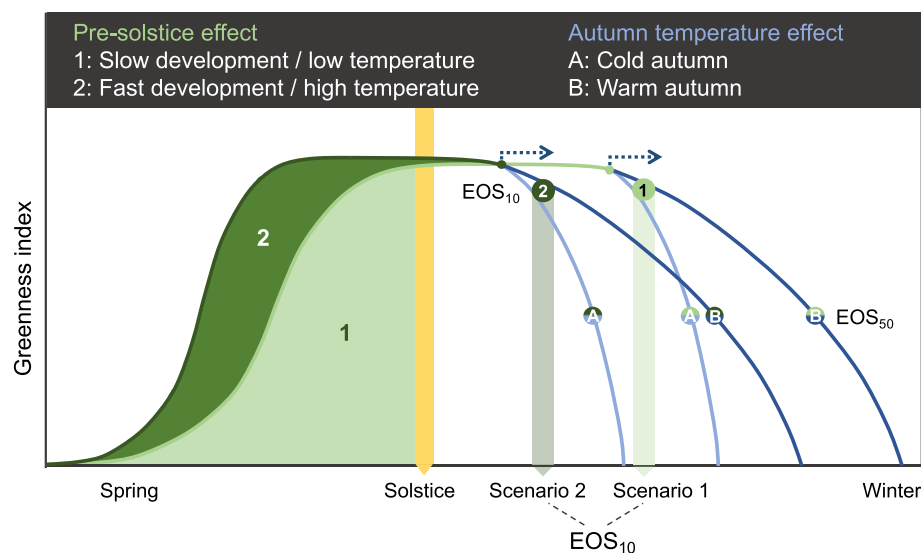

Fig. 1. Conceptual model of autumn phenological responses to pre-solstice and post-solstice growth and temperature (solstice-as-phenology-switch hypothesis). The onset of autumnal senescence was estimated in this study as the date when the greenness index last dropped by >10% of the seasonal maximum (EOS$_{10}$). In northern forests, stem growth, development rates, and photosynthetic capacity are highest before the summer solstice and decline with shortening days (*14–16*). Interannual variation in EOS$_{10}$ is a function of pre-solstice growth and development, with later EOS$_{10}$ in years with slow development and low temperature before the solstice (scenario 1) and earlier EOS$_{10}$ in years with fast development and high temperature (scenario 2). The progression of leaf senescence varies with autumn temperature, with faster chlorophyll breakdown in cold-autumn years (scenario A) than in warm-autumn years (scenario B). The dates of 50% chlorophyll loss (EOS$_{50}$) are therefore driven by pre- and post-solstice effects, whereas EOS$_{10}$ dates are mainly driven by pre-solstice effects. An earlier start of senescence in high-activity years (scenario 2) also predicts that trees will become sensitive to autumn cooling earlier than in low-activity years (see blue arrows).

[1]Institute of Integrative Biology, ETH Zurich (Swiss Federal Institute of Technology), 8092 Zurich, Switzerland. [2]Department of Civil and Environmental Engineering, Massachusetts Institute of Technology, Cambridge, MA 02139, USA. [3]Department of Biology, Washington University in St. Louis, Saint Louis, MO 63130, USA. [4]Department of Experimental Plant Biology, Charles University in Prague, CZ 128 44 Prague, Czech Republic. [5]WSL Swiss Federal Institute for Forest, Snow and Landscape Research, 8903 Birmensdorf, Switzerland. [6]College of Water Sciences, Beijing Normal University, Beijing 100875, China. [7]Institute of Geography, University of Bern, 3012 Bern, Switzerland. [8]Oeschger Centre for Climate Change Research, University of Bern, 3012 Bern, Switzerland.
*Corresponding author. Email: constantin.zohner@gmail.com

autumns (*30*, *31*) (Fig. 1, scenario A versus B). Continued acceleration of early-season growth and development under climate warming (*4*, *5*, *32*, *33*) might thus cause an ever earlier EOS onset, whereas the progression of senescence should be slowed down by warmer autumns (*22*, *23*), lengthening the overall senescence period. This leads to four fundamental predictions that were tested in this study: (i) Enhanced pre-solstice temperature and vegetation activity drives an earlier senescence onset (Fig. 1, scenario 1 versus 2). (ii) Growth and temperature effects on senescence dates reverse around the time of the summer solstice. (iii) Autumn temperature affects the speed of senescence, delaying its later stages (scenario A versus B), but has little effect on its start. (iv) The date when trees become sensitive to autumn cooling (blue arrows in Fig. 1) has advanced over recent decades because of an earlier onset of senescence.

To test these hypotheses, we combined phenology data from satellite observations across Northern Hemisphere temperate and boreal forests (*34*), ground observations from European (*35*) and American (*36*) deciduous trees, eddy covariance flux tower measurements (*37*), and controlled experiments on European beech (*38*). Seasonal vegetation activity was estimated using direct measurements of leaf-level gas exchange and ecosystem carbon fluxes (*37*), as well as photosynthesis models [satellite-derived gross primary productivity (GPP) (*39*) and the Lund–Potsdam–Jena General Ecosystem Simulator (LPJ-GUESS) model (*9*)]. We then ran linear models to test for the monthly and seasonal effects of photosynthesis, temperature, shortwave radiation, and water availability on EOS dates. The satellite data allowed us to differentiate between the onset of senescence and its progression by analyzing the dates when greenness had dropped by 10% (EOS$_{10}$) or 50% (EOS$_{50}$) relative to the seasonal maximum. The experiments allowed us to directly test for seasonal variation in the effects of air temperature and radiation. Finally, we mapped the relative effects of early-season vegetation activity and late-season climate across Northern Hemisphere forests to test for possible biogeographic patterns in the drivers of autumn senescence.

Effect of temperature and vegetation activity on senescence dates reverses after the summer solstice

Satellite-based phenology data (Figs. 2 and 3 and figs. S1 to S3), European (Fig. 4) and American (fig. S4) ground observations, flux tower measurements (figs. S5 and S6), and experiments (fig. S7) all revealed a consistent advancing effect of pre-solstice (i.e., before 21 June) temperature and productivity on EOS dates, which declined after the summer solstice. Thus, across 84% of the northern forest area [18% (Fig. 3C) and 22% (fig. S1C) significant at $P < 0.05$], increased pre-solstice daytime temperature (T_{day}) and photosynthesis led to an earlier onset of senescence: each 1°C increase in pre-solstice temperature resulted, on average, in 1.9 ± 0.1 (mean ± 2 SE) days earlier EOS$_{10}$ (Fig. 3D). Similarly, each
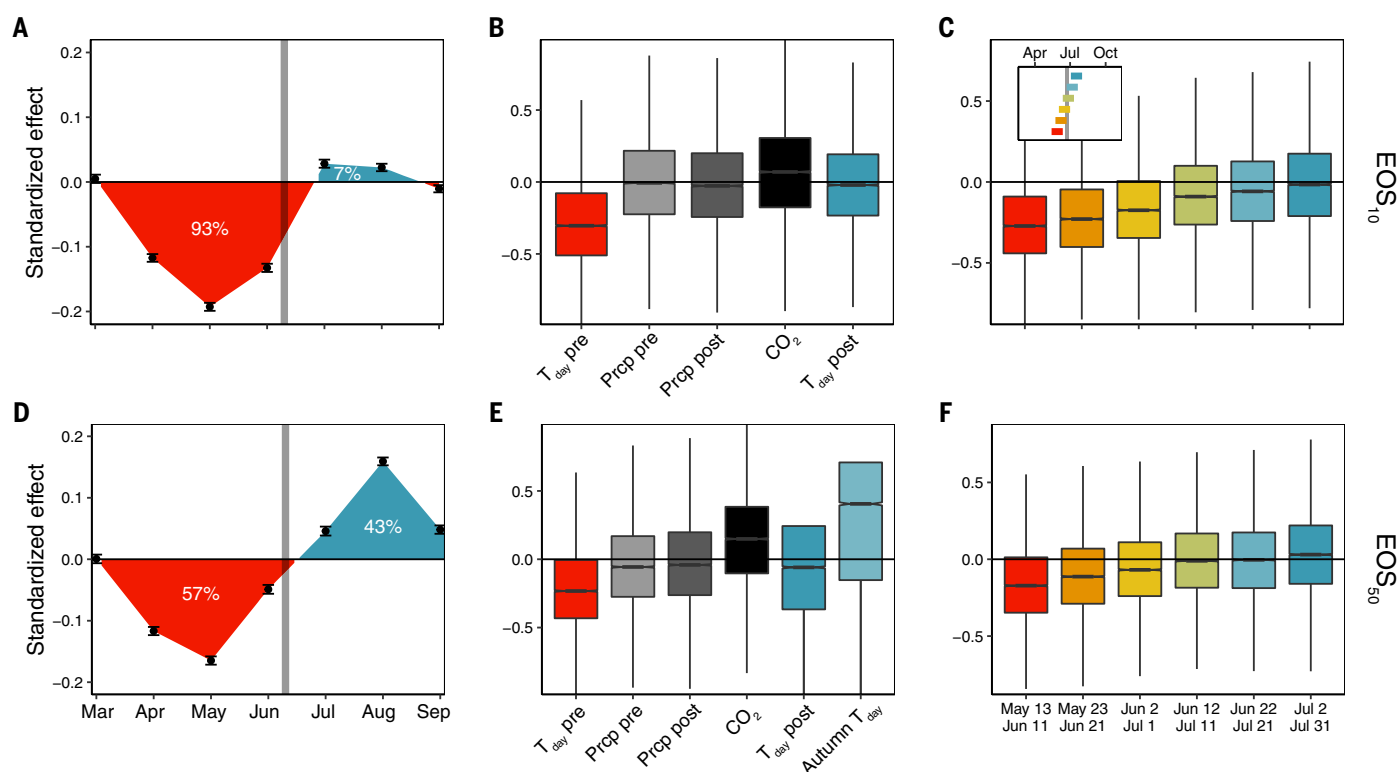
Fig. 2. Effect of temperature on the timing of autumn senescence in northern forests reverses after the summer solstice. Autumn phenology is represented as EOS$_{10}$ (A to C) or EOS$_{50}$ (D to F) dates from satellite observations (see Fig. 3A). (**A** and **D**) Relationship between mean monthly T_{day} and EOS dates (means ± 95% confidence ranges) from multiple linear regression models. Percentages reflect the total positive and negative areas under the curve, meaning the relative advancing versus delaying effects of seasonal T_{day}. (**B** and **E**) Effects of pre-solstice daytime temperature (T_{day} pre; 20 March to solstice) and precipitation (Prcp pre), post-solstice daytime temperature (T_{day} post; solstice to mean pixel-level EOS date) and precipitation (Prcp post), and atmospheric CO_2 on EOS dates [(E) additionally includes the effect of autumn T_{day}]. (**C** and **F**) The univariate effects of 1-month-long T_{day} intervals around the summer solstice [13 May to 11 June, 23 May to 21 June, 2 June to 1 July, 12 June to 11 July, 22 June to 21 July, and 2 July to 31 July; the inset in (C) illustrates the time of year of each period, and the gray vertical line represents the summer solstice] on EOS dates. Analyses show relative effect sizes from pixel-level linear models. To examine relative effect sizes, both predictor and dependent variables were standardized by subtracting their mean and dividing by one standard deviation before analysis.
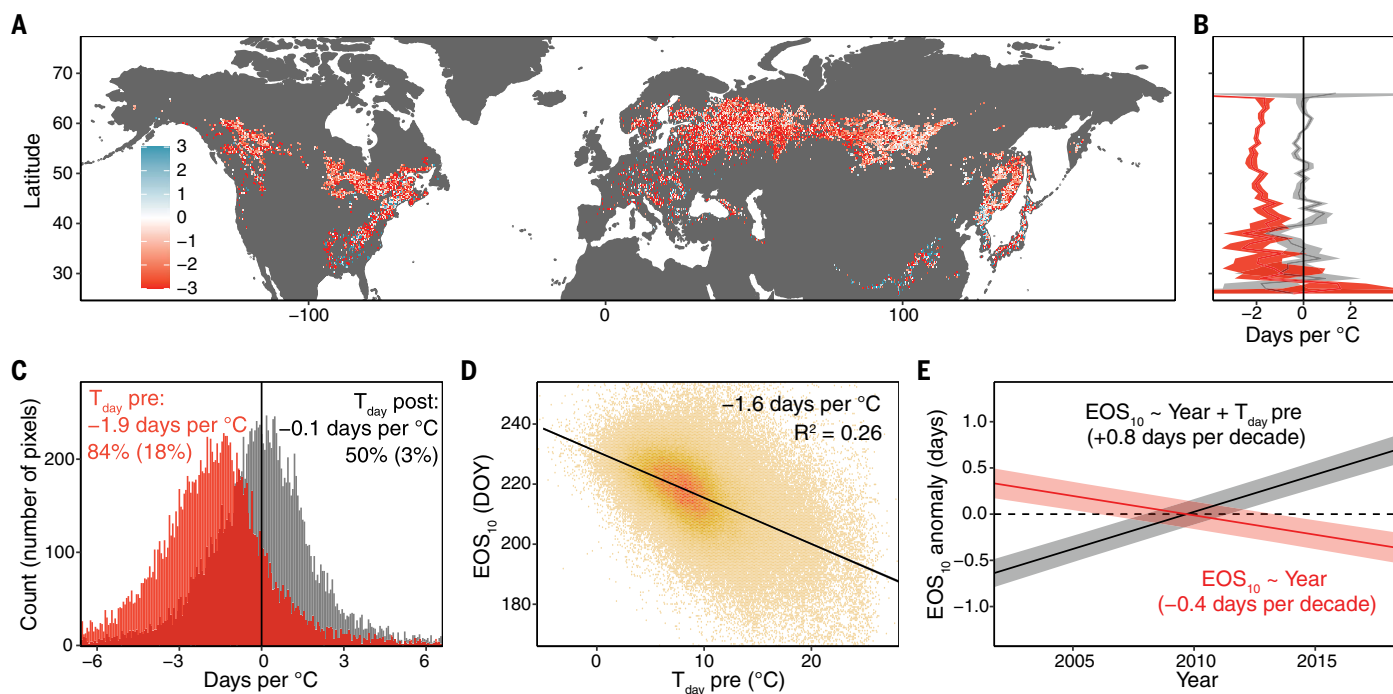
Fig. 3. Satellite observations reveal consistent advances in the onset of senescence (EOS$_{10}$) across northern forests in response to increased pre-solstice temperature. (**A**) Map showing the effects of pre-solstice (20 March to solstice) T_{day} on EOS$_{10}$ timing at 0.25° resolution from linear models, including pre-solstice T_{day} and post-solstice (solstice to mean pixel-level EOS date) T_{day} as predictor variables. Red pixels indicate an earlier EOS$_{10}$ under increased pre-solstice T_{day}, blue pixels indicate a delayed EOS$_{10}$. (**B**) Regression coefficient means and 95% confidence ranges summarized for each degree latitude (pre-solstice effects in red, post-solstice effects in black). (**C**) The distribution of the pre-solstice and post-solstice T_{day} effects across all pixels. Mean pre- and post-solstice T_{day} regression coefficients and the percentage of pixels with an advancing pre-solstice T_{day} effect or delaying post-solstice T_{day} effect shown as red and black text, respectively (percentage of significant pixels at $P < 0.05$ in brackets). (**D**) Partial effect of pre-solstice T_{day} on EOS$_{10}$ dates, controlling for year (fixed effect) and site (random effect). (**E**) Temporal trends in EOS$_{10}$ anomalies (means ± 95% confidence ranges) from mixed-effects models with year as a single fixed effect (red line and equation) or including pre-solstice T_{day} as an additional fixed effect (black line and equation). Pixels were treated as grouping variables of random intercepts.

10% increase in pre-solstice photosynthesis resulted in 3.6 ± 0.1 days earlier EOS$_{10}$ (satellite data; fig. S1) or 3.7 ± 1.2 days earlier PD$_{25}$ (date when photosynthesis had dropped by 25% relative to the seasonal maximum according to flux tower data; fig. S6). A significant delaying effect of pre-solstice temperature and photosynthesis was found for <1% of northern forest pixels.

Post-solstice temperature had a small effect on the onset of senescence (see Figs. 2, A and B, and 5A for EOS$_{10}$ dates, and fig. S8, A and B, for EOS$_{start}$ dates as an alternative measure of senescence onset) but prolonged its duration (number of days from EOS$_{10}$ to EOS$_{85}$, EOS$_{10}$ to EOS$_{50}$, or EOS$_{50}$ to EOS$_{85}$) by 1.3 to 3.5 days per °C (fig. S9), explaining the large effect of autumn temperatures on EOS$_{50}$ dates (Fig. 2, D and E, and fig. S2, C to E, for satellite observations and Figs. 4 and 5C for European plots). Precipitation and CO_2 levels had comparatively small effects (Fig. 2, B and E, and fig. S10).

The reversal of the effects of air temperature and vegetation activity on EOS dates after the summer solstice was consistent across (i) all

EOS metrics used here, that is, the onset of senescence (EOS$_{10}$ or EOS$_{start}$; Fig. 2, A to C, and fig. S8) and mid-senescence (EOS$_{50}$; Fig. 2, D to F); (ii) continents and forest types (fig. S11); and (iii) a set of alternative variables linked to growing-season activity and development, namely T_{day} (Fig. 3 and fig. S2) and photosynthetic activity (figs. S1 and S3). Along the full latitudinal gradient (30°N to 65°N) studied here, the period during which vegetation productivity had an advancing effect on EOS$_{10}$ dates consistently ended after the solstice, at ~26 June (fig. S12). The effect reversal after the summer solstice was further supported by an analysis that used 10-day moving steps around the solstice (Fig. 2, C and F). To further test for the importance of separating pre- and post-solstice variables for EOS predictions, we ran leave-one-out cross-validation of models that included (i) only pre-solstice, (ii) only post-solstice, or (iii) both types of variables as predictors of EOS dates (*38*). In full agreement with our hypothesis (Fig. 1), the onset of senescence (EOS$_{10}$) was better explained by pre-solstice than by post-solstice variables, and the full model—including both

pre-and post-solstice variables—showed only slightly better performance than the pre-solstice model (fig. S13, A and D). Because autumn temperature modulates the progression of senescence, EOS$_{50}$ dates were slightly better explained by post-solstice than by pre-solstice variables, with the combination of both variables yielding the best predictions (fig. S13, B, C, E, and F).

In line with the satellite observations, high pre-solstice temperature and productivity correlated with advanced EOS$_{50}$ dates in the European and American plot data, across all species (Fig. 4B and fig. S4) and across a set of alternative variables [T_{day} (Fig. 4) and LPJ-GUESS model–derived photosynthesis (fig. S15)]. On the basis of these findings, we ran multivariate mixed models for the European plot data, including pre-solstice and post-solstice (solstice to mean EOS$_{50}$) temperature or photosynthesis and precipitation, CO_2 levels, and autumn nighttime temperature (autumn T_{night}) to determine their relative importance. Pre-solstice temperature (or photosynthesis) had the strongest advancing effect on EOS$_{50}$ dates, whereas autumn T_{night} had the strongest
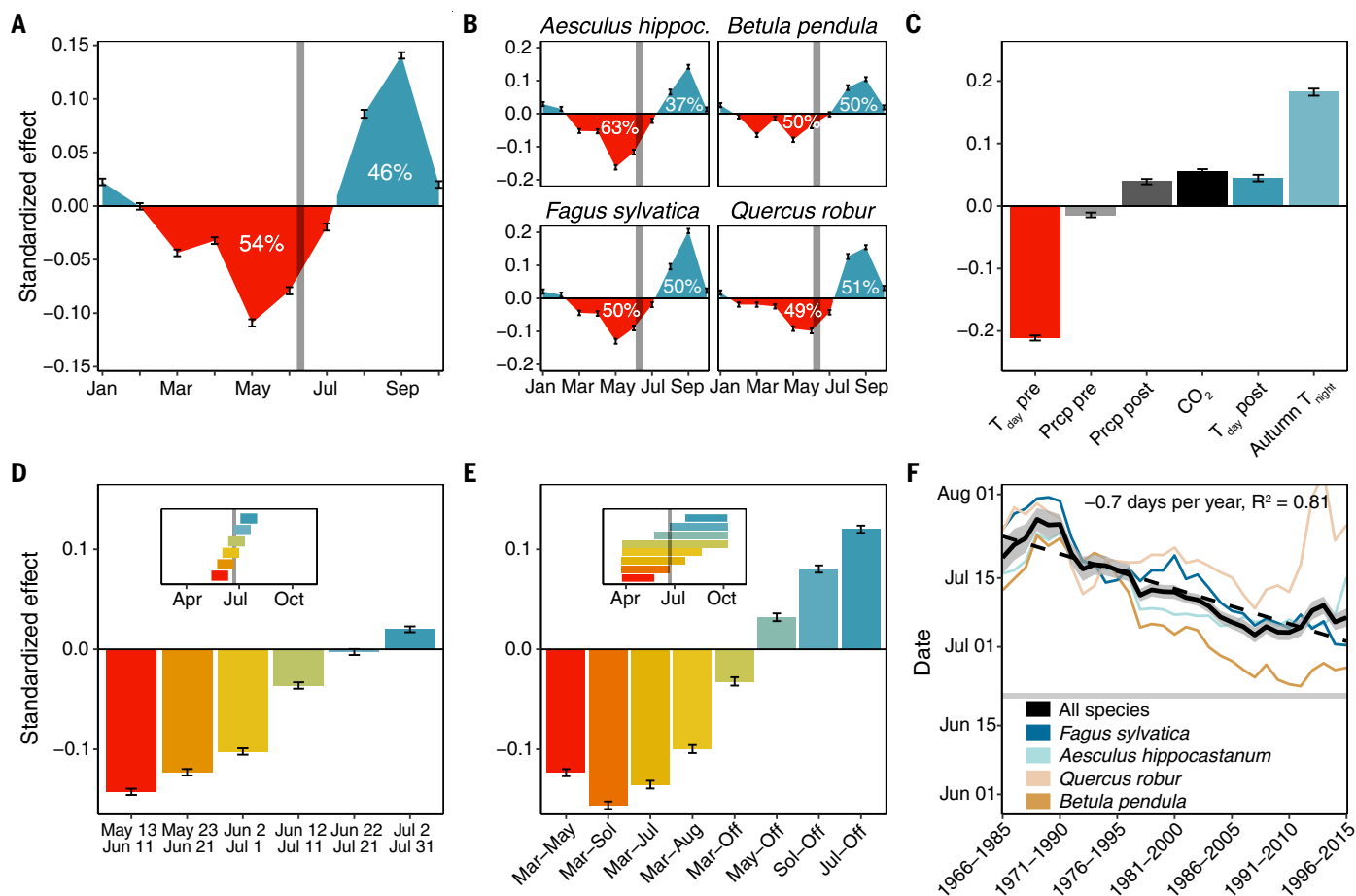
Fig. 4. The seasonal effects of temperature on interannual variation in mid-senescence (EOS$_{50}$ dates) from European long-term observations (PEP725 data). (**A**) Effects of monthly (January to October) T_{day} on autumn senescence dates. Percentages reflect the total positive and negative areas under the curve, meaning the relative advancing versus delaying effects of temperature. (**B**) Species-level results. (**C**) The relative effects of pre-solstice (20 March to solstice) and post-solstice (solstice to mean EOS$_{50}$) temperature, pre-solstice and post-solstice precipitation, atmospheric CO_2, and autumn nighttime temperature (Autumn T_{night}). (**D**) Effects of 1-month-long temperature intervals around the summer solstice (13 May to 11 June, 23 May to 21 June, 2 June to 1 July, 12 June to 11 July, 22 June to 21 July, and 2 July to 31 July; see inset), including the respective temperature interval as a single fixed effect.

(**E**) The effects of mean temperature from 20 March to 22 May (Mar–May), 20 March to solstice (Mar–Sol), 20 March to 21 July (Mar–Jul), 20 March to 20 August (Mar–Aug), 20 March to mean EOS$_{50}$ (Mar–Off), 22 May to mean EOS$_{50}$ (May–Off), solstice to mean EOS$_{50}$ (Sol–Off), and 21 July to mean EOS$_{50}$ (Jul–Off), including the respective temperature interval as fixed effect. (**F**) Moving-window analysis, showing the "reversal" dates when the temperature effect switches from negative to positive for each 20-year time period from 1966 to 2015 [based on monthly correlations; see (A) to (C)]. On average, the reversal date advanced by 0.7 days per year. Analyses show effect size means ± 2 SE from linear mixed models, including time series and species [(A) and (C) to (E)] or only time series [(B) and (F)] as random effects, with both predictor and dependent variables standardized. R^2, coefficient of determination.

delaying effect on EOS$_{50}$ dates, with both effects being more than three times greater than that of precipitation and atmospheric CO_2 (Fig. 4C). EOS predictions showed that the full model representing both pre- and post-solstice effects captured within-site EOS$_{50}$ trends in response to mean annual temperature (advance of 0.4 ± 0.1 days per °C increase in mean annual temperature; fig. S16). In contrast, a model representing only post-solstice temperature and precipitation predicted delays of 0.7 ± 0.1 days per °C, whereas a pre-solstice model predicted advances of 0.9 ± 0.1 days per °C. These findings demonstrate that information on both pre- and post-solstice cli-

mate is necessary to reproduce the observed EOS$_{50}$ responses to rising temperature.

Ongoing trends toward an earlier start, slowed progression, and later end of senescence

Our finding that the onset of senescence is driven by pre-solstice vegetation activity and development, while the speed of its progression depends on autumn temperature (fig. S9), suggests that global warming leads to an earlier start and slowed progression of senescence (scenario 2B in Fig. 1). Indeed, across all analyzed northern forest pixels, the onset of senescence (EOS$_{10}$ date) has advanced by an average of −0.4 ± 0.1 days per decade between

2001 and 2018 (Fig. 3E), in parallel with increased pre-solstice vegetation productivity (fig. S14, A and B), with the strongest advances in EOS$_{10}$ dates found for regions with the largest increase in pre-solstice productivity (fig. S14K). When removing the effect of pre-solstice temperature or photosynthesis on senescence onset by including either variable as a fixed effect in addition to year, the model instead predicted delays in EOS$_{10}$ dates of 0.8 to 1.4 days per decade (Fig. 3E and fig. S1E), underscoring how strongly temperature-driven pre-solstice vegetation activity affects the start of senescence. The warmer autumns (fig. S14, I and J) are instead slowing the progression of
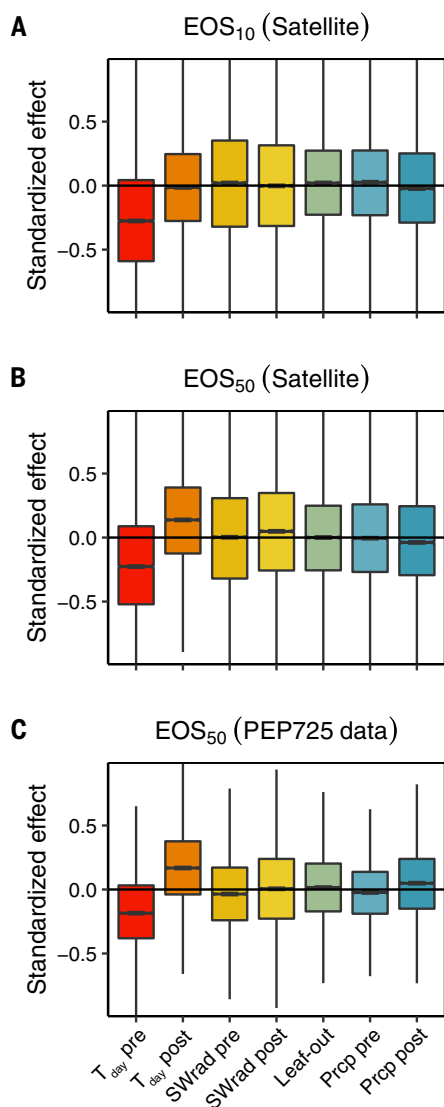
A

EOS$_{10}$ (Satellite)

B

EOS$_{50}$ (Satellite)

C

EOS$_{50}$ (PEP725 data)

Fig. 5. The effects of temperature, radiation, spring leaf-out dates, and precipitation on inter-annual variation in the timing of EOS$_{10}$ and EOS$_{50}$. Panels show results for satellite-derived EOS$_{10}$ dates (**A**), satellite-derived EOS$_{50}$ dates (**B**), and ground-sourced EOS$_{50}$ dates (**C**). All linear models include mean T_{day} and shortwave radiation (SWrad) and the sums of precipitation (prcp) from 20 March to 21 June (pre-solstice) and from 22 June to the mean EOS date of each time series (post-solstice), as well as spring leaf-out dates, as predictor variables. Models were run at the pixel level [(A) and (B)] or individual level (C), and boxplots show the spread of effect sizes. All variables were standardized to allow for direct effect size comparison.

senescence, leading to delays in EOS$_{50}$ dates (fig. S2G), especially in regions with the largest increases in autumn temperature (Fig. S14M).

The offsetting effect of pre-solstice vegetation activity on autumn warming–induced delays in EOS$_{50}$ is also apparent in regional

trends over the past 70 years (time series and species as random effects; fig. S17). On average, European EOS$_{50}$ dates have been delayed by only +0.35 ± 0.02 days per decade (fig. S17B). By contrast, when keeping pre-solstice productivity constant by including it as a fixed effect in addition to year, the model predicts a delay of +0.81 ± 0.03 days per decade (fig. S17D), showing that the increase in pre-solstice vegetation productivity has offset up to ~60% of the delay in EOS$_{50}$ that would have occurred had pre-solstice productivity not increased. This explains why EOS$_{50}$ delays have contributed only ~15% (2.4 ± 0.2 days) to the 16.7 ± 0.4 day–long extension of the growing season that has occurred over the past 70 years (fig. S17, A and B).

The longer senescence duration (fig. S9) and delayed EOS$_{50}$ dates (when greenness has dropped by 50%) under warmer autumns reveal how autumn temperature modulates senescence (Figs. 4C and 5, B and C, and fig. S18, C and D). However, if increased pre-solstice vegetation development (fig. S14A) is the main driver of an earlier onset of EOS, one should find an ever earlier susceptibility of trees to autumn cooling. We tested this by using temporal moving-window analyses on the European long-term observations and found that the effect reversal dates, at which increased temperature and productivity start to be associated with delayed EOS$_{50}$ dates, have indeed advanced, by an average of –0.7 to –1.0 days per year (Fig. 4F and fig. S15F or fig. S19B for a shorter moving window). This is also reflected in the moving windows of monthly effect sizes, which show that July photosynthesis has become more strongly associated with delayed EOS$_{50}$ dates over recent decades (fig. S19C). As an alternative method of determining when autumn cooling starts driving senescence progression, we modeled the autumn period best explaining EOS$_{50}$ dates and found that it has advanced by –0.20 ± 0.07 days per year for the 1966–2015 period (fig. S20A) or by –0.43 ± 0.09 days per year for the 1981–2015 period (fig. S20B). This earlier start of the period when trees react to autumn cooling provides further evidence for an earlier onset of senescence in response to increased early-season development.

An important consideration of our autumn senescence model presented in Fig. 1 is that the effect reversal date—the compensatory point of the advancing and delaying effects—should be flexible despite day length likely triggering the initial decline in the advancing effect after the summer solstice (14, 15, 17). This is because the actual reversal date of the antagonistic effects, meaning the period when trees become sensitive to cooling in late summer, is a function of warming and development before the summer solstice, which will vary (Fig. 1). Involvement of day length and a flexible effect

reversal date are therefore not mutually exclusive ideas but rather necessary components of the same model.

Factors governing the link between pre-solstice temperature and senescence onset

Previous research on European deciduous trees has suggested a negative feedback between growing-season productivity and autumn phenology, with increased productivity driving earlier senescence (9). The data analyzed here now reveal that the productivity before the summer solstice is indeed linked to earlier senescence dates and that this holds across the entire Northern Hemisphere temperate and boreal forest biome, implying a widespread constraint on future growing-season extensions in response to global warming. To disentangle the environmental drivers of this feedback, we ran multiple linear regression models that included air temperature, solar radiation, water availability, and spring leaf-out dates as predictor variables, all of which have been shown to affect leaf senescence dates (9, 11, 20, 26, 28, 40) (Fig. 5 and figs. S21 or S22 using soil moisture instead of precipitation to represent water availability). Across the majority of pixels or sites, pre-solstice temperature was the main driver of EOS$_{10}$ dates (Fig. 5A), whereas EOS$_{50}$ dates were driven by both pre- and post-solstice temperatures, with opposite effect directions (Fig. 5, B and C). This suggests that temperature-driven development and growth—rather than radiation-induced leaf aging, drought, or leaf-out per se (i.e., constrained leaf life span)—are driving the advancing effect of early-season vegetation activity on autumn phenology.

To further isolate the mechanisms driving the discovered reversal of the effects of global warming around the summer solstice, we conducted an experiment on a dominant European tree species (*Fagus sylvatica*), in which we cooled (chamber temperature set to 10°C during the day and 5°C at night) and shaded (~84% light reduction) saplings during different times of the season. Pre-solstice temperature again had a strong advancing effect on autumn phenology, with cooling of trees in June causing a delay in EOS$_{10}$ and EOS$_{50}$ dates of +16.5 ± 6.6 days and +10.2 ± 2.5 days (mean ± SE), respectively. Cooling in July had no effect, and August cooling tended to advance EOS dates (figs. S7A and S23A), in full agreement with the global-scale remote sensing data and the ground observations. The effect of shading was small before the summer solstice and most pronounced during July—the month with the highest mean daily radiation and temperature—with EOS$_{50}$ delayed by +6.5 ± 2.8 days under shade conditions. Radiation effects thus followed a different seasonal pattern than temperature, supporting a direct effect of radiation on leaf aging (26, 29). Summer

photosynthesis was equally reduced in both the shade and the cooling treatments by 52 to 72% compared with the control (fig. S24). That pre-solstice temperature, but not pre-solstice light availability, affected EOS dates provides further support for the idea that accelerated development and growth under warmer temperatures, rather than photosynthesis- or radiation–induced leaf aging, are the main drivers of the pre-solstice effects on senescence dates. Yet given that both plant developmental speed (tissue expansion and meristematic activity) and photosynthesis early in the season are strongly driven by temperature (*41*), both processes are linked, and pre-solstice GPP therefore appears to be a reliable proxy of this effect (fig. S1).

An important future avenue will be to disentangle the relative roles of developmental processes within leaves (*42*) versus growth processes in the rest of the plant (*25, 41*) in driving earlier senescence under increased pre-solstice temperatures. That pre-solstice temperatures and productivity advanced senescence even in species with continuous leaf production throughout the season, such as *Betula pendula* (Fig. 4B and fig. S15B), suggests that leaf development and longevity cannot be the sole drivers, implying involvement of growth (sink) processes in other organs, including wood, roots, and buds. This idea was further supported by a second experiment in which we tested the response of primary growth cessation (bud set) to pre- and post-solstice warming. The results showed that pre-solstice warming (22 May to 21 June) advanced bud set in *F. sylvatica* by 4.4 ± 1.8 days, whereas post-solstice warming (22 June to 21 July) delayed bud set by 4.9 ± 1.8 days (fig. S25), consistent with an effect reversal after the summer solstice. The negative effect of warmer pre-solstice temperatures on growing-season duration is therefore not limited to leaf development and life span (*23, 42, 43*), suggesting an important role of overall plant growth and sink activity before the solstice in determining autumn growth cessation and leaf senescence (*14, 16, 17, 41*).

The observed EOS advances under elevated pre-solstice temperature and growth may additionally be linked to availability of soil resources throughout the growing season. Optimal growth conditions in spring (high temperatures and sufficient precipitation) may deplete nitrogen availability to trees, which in turn may drive early bud set and senescence (*25, 26, 44*). This effect may be further enhanced by increased C:N ratios of leaves under rising atmospheric CO_2, causing microbial immobilization and reduced nitrogen accessibility (*45, 46*).

Conclusions

Our investigation of the seasonal drivers of autumn phenology shows a consistent reversal after the summer solstice in the effects of climate warming on leaf senescence (i) across large biogeographic ranges with varying pre-solstice growth (satellite data); (ii) in multiple, broad-ranged tree species with different spring phenologies (ground data); (iii) in eddy covariance measurements; and (iv) under controlled experimental conditions. These findings reveal important constraints on growing-season length and photosynthetic activity, whereby earlier and enhanced activity before the summer solstice drives earlier photosynthetic declines, primary growth cessation, and senescence in autumn. The seasonal control on EOS by air temperature and vegetation activity may be mediated by the annual day-length cycle (*15, 17*) and nutrient availability (*26, 44*). Year-to-year differences in the onset and progression of autumn senescence thus emerge as the result of a complex synchronization between trees' developmental states, seasonal variation in the circadian rhythm, and climate fluctuations. This mediation by the annual day-length cycle provides a unifying framework to explain previous results, in which the magnitude and direction of climate warming effects on autumn phenology varied (*9, 12, 22, 23, 33, 47–50*), largely because studies did not disentangle pre- and post-solstice variables. It now is clear that warmer temperatures and increased vegetation activity before the summer solstice drive an earlier onset of senescence, whereas, in agreement with previous studies (*12, 47, 51*), warmer temperatures after the solstice slow down the progression of senescence, predicting that senescence will continue to start earlier but progress more slowly.

The reversal in how trees respond to temperature during the summer likely evolved as an adaptation to seasonal climates with harsh winters because it allows plants to reliably anticipate the progression of the seasons and prepare for winter dormancy long before the temperature starts dropping (*19*). The solstice switch in trees' physiological responsiveness to temperature calibrates their seasonal rhythms and mediates how they react to warm or cool temperatures, now and in the future. This enables trees to initiate tissue maturation and the physiological processes of leaf senescence and nutrient resorption (*15*) in a fine-tuned balance between source and sink dynamics. Improved models of plant development and growth under climate change will need to incorporate the reversal of warming effects after the summer solstice.

Methods summary
Satellite observations
Start-of-season (SOS) and EOS dates for Northern Hemisphere forests from 2001 to 2018 came from the MODIS Global Vegetation Phenology product (*34*). SOS was defined as the date when satellite-derived greenness had reached 15% of its annual maximum. EOS was defined as the date when greenness had decreased by 10% (EOS_10), 50% (EOS_50), or 85% (EOS_85), representing the start of senescence, mid-greendown, and dormancy, respectively. As an alternative measure of the start of senescence, we used the VIIRS/NPP Land Cover Dynamics product (*52*), which uses a breakpoint algorithm to define the onset of greendown. Information on climate came from (*53*), and GPP came from the MODIS GPP product (*39*). We included GPP, T_{day}, T_{night}, shortwave radiation, CO_2 levels, precipitation, soil moisture, and SOS dates as covariates in our analyses.

To investigate the seasonal effects of temperature, photosynthesis, shortwave radiation, and water availability on the timing of EOS_50 dates, we aggregated data for different periods before and after the summer solstice. For each time series, we also determined the optimal autumn interval for which temperature explains most of the variation in EOS_50 dates. We quantified the importance of each covariate in driving interannual variation in EOS dates with pixel-level linear models (Figs. 2 and 3). To approximate the end date of the period during which early-season vegetation activity had an advancing effect on the onset of senescence, we tested the correlation between different GPP periods (always beginning at the SOS date) and EOS_10 dates (fig. S12). To test for decadal-scale temporal trends in EOS dates, we ran mixed-effects models including only year or year and pre-solstice temperature (Fig. 3, D and E) or GPP (fig. S1, D and E) as fixed effects and treating pixels as grouping variables of random intercepts.

Ground observations
Ground data on 396,411 EOS dates of four dominant tree species in central Europe between 1951 and 2015 came from the Pan European Phenology Project (*35*). Climate data for the same period were obtained from the Global Land Data Assimilation System (*53*). The EOS_50 corresponded to the date when 50% of leaves had lost their green color. We included photosynthesis, T_{day}, T_{night}, shortwave radiation, CO_2 levels, precipitation, soil moisture, and spring leaf-out dates as covariates in our analyses. Daily photosynthesis was derived from the LPJ-GUESS photosynthesis model (*54*). As for the satellite observations, data were aggregated for monthly and longer periods before and after the summer solstice, and we also determined the optimal autumn interval for which temperature explains most of the variation in EOS_50 dates.

The importance of these variables in driving EOS dates was then evaluated with linear mixed models, including time series (unique site and species combination) and species random effects. Our final model included fixed

effects of pre- and post-solstice T_{day} (Fig. 4C) or photosynthesis (fig. S15C), as these variables emerged as the strongest drivers of EOS dates.

To test whether the relative effects of variables have been changing over the past decades, we ran the mixed models separately for each 20-year (or 15-year) time period from 1966 to 2015 (or 1980 to 2015). To estimate the date at which the effect of temperature and photosynthesis reverses, we conducted moving-window analyses of the monthly temperature and photosynthesis effects. Additionally, we estimated the day at which autumn temperature starts driving senescence progression by calculating the autumn period for which temperature best explained variation in EOS_{50} dates for each moving window (fig. S20). We additionally analyzed direct observations of EOS_{50} dates for 10 North American tree species from 1991 to 2019 from the Phenology of Woody Species at Harvard Forest dataset (36) (fig. S4).

Flux tower measurements

Eddy covariance data from 10 temperate forest (broadleaf deciduous/mixed) sites with >9 years of data were gathered from the FLUXNET2015: CC-BY-4.0 dataset (37). To represent the onset dates of photosynthesis declines (PD) in late summer, we extracted the day of year on which GPP last dropped below 10% (PD_{10}; fig. S5) or 25% (PD_{25}; fig. S6) of maximum annual GPP. We then tested for the relationships between monthly (April to September) GPP estimates and PD_{10} or PD_{25} dates by running mixed-effects models, including site as a random effect.

Experiments

In the first experiment, we tested for the effects of seasonal variation in temperature and light on EOS dates. We exposed 3-year-old *F. sylvatica* trees to cooling or shading conditions during four 1-month-long periods (from May to August). In the cooling treatments, trees experienced a nighttime temperature of 5°C and a daytime temperature of 10°C. In the shading treatments, trees were exposed to an ~84% reduction in incoming radiation. Individual leaf senescence dates were defined as the day of year when chlorophyll content last dropped by 10% (EOS_{10}) or 50% (EOS_{50}) of the maximum chlorophyll content in summer. Leaf net photosynthesis was measured with a portable infrared gas analyzer (LI-6800, LI-COR Biosciences, Lincoln, NE). To test for differences in leaf senescence dates among treatments, we ran multivariate linear models including temperature and shade treatments as categorical variables.

In the second experiment, we tested the effects of pre- and post-solstice warming on bud set dates by exposing 4-year-old *F. sylvatica* trees to cooling conditions (8°C during day

and night) during 1-month-long periods before and after the solstice. Bud set was defined as the date when the buds of an individual had reached >90% of their final length (23), indicating aboveground primary growth cessation (23, 55). To test for differences in bud set dates and autumn bud growth rates among treatments, we ran mixed-effects models including treatment as categorical fixed effect and bud types (apical versus lateral) as a random effect.

REFERENCES AND NOTES

1. I. Chuine, Why does phenology drive species distribution? *Philos. Trans. R. Soc. London Ser. B* **365**, 3149–3160 (2010). doi: 10.1098/rstb.2010.0142; pmid: 20819809
2. S. S. Renner, C. M. Zohner, Climate change and phenological mismatch in trophic interactions among plants, insects, and vertebrates. *Annu. Rev. Ecol. Evol. Syst.* **49**, 165–182 (2018). doi: 10.1146/annurev-ecolsys-110617-062535
3. A. D. Richardson *et al.*, Climate change, phenology, and phenological control of vegetation feedbacks to the climate system. *Agric. For. Meteorol.* **169**, 156–173 (2013). doi: 10.1016/j.agrformet.2012.09.012
4. T. F. Keenan *et al.*, Net carbon uptake has increased through warming-induced changes in temperate forest phenology. *Nat. Clim. Chang.* **4**, 598–604 (2014). doi: 10.1038/nclimate2253
5. C. M. Zohner, L. Mo, T. A. M. Pugh, J. F. Bastin, T. W. Crowther, Interactive climate factors restrict future increases in spring productivity of temperate and boreal trees. *Glob. Change Biol.* **26**, 4042–4055 (2020). doi: 10.1111/gcb.15098; pmid: 32347650
6. Y. Vitasse *et al.*, The great acceleration of plant phenological shifts. *Nat. Clim. Chang.* **12**, 300–302 (2022). doi: 10.1038/s41558-022-01283-y
7. N. Delpierre *et al.*, Modelling interannual and spatial variability of leaf senescence for three deciduous tree species in France. *Agric. For. Meteorol.* **149**, 938–948 (2009). doi: 10.1016/j.agrformet.2008.11.014
8. A. Menzel, P. Fabian, Growing season extended in Europe. *Nature* **397**, 659 (1999). doi: 10.1038/17709
9. D. Zani, T. W. Crowther, L. Mo, S. S. Renner, C. M. Zohner, Increased growing-season productivity drives earlier autumn leaf senescence in temperate trees. *Science* **370**, 1066–1071 (2020). doi: 10.1126/science.abd8911; pmid: 33243884
10. L. Chen *et al.*, Leaf senescence exhibits stronger climatic responses during warm than during cold autumns. *Nat. Clim. Chang.* **10**, 777–780 (2020). doi: 10.1038/s41558-020-0820-2
11. T. F. Keenan, A. D. Richardson, The timing of autumn senescence is affected by the timing of spring phenology: Implications for predictive models. *Glob. Change Biol.* **21**, 2634–2641 (2015). doi: 10.1111/gcb.12890; pmid: 25662890
12. G. Liu, X. Chen, Q. Zhang, W. Lang, N. Delpierre, Antagonistic effects of growing season and autumn temperatures on the timing of leaf coloration in winter deciduous trees. *Glob. Change Biol.* **24**, 3537–3545 (2018). doi: 10.1111/gcb.14095; pmid: 29460318
13. S. Piao *et al.*, Net carbon dioxide losses of northern ecosystems in response to autumn warming. *Nature* **451**, 49–52 (2008). doi: 10.1038/nature06444; pmid: 18172494
14. S. Rossi *et al.*, Conifers in cold environments synchronize maximum growth rate of tree-ring formation with day length. *New Phytol.* **170**, 301–310 (2006). doi: 10.1111/j.1469-8137.2006.01660.x; pmid: 16608455
15. W. L. Bauerle *et al.*, Photoperiodic regulation of the seasonal pattern of photosynthetic capacity and the implications for carbon cycling. *Proc. Natl. Acad. Sci. U.S.A.* **109**, 8612–8617 (2012). doi: 10.1073/pnas.1119131109; pmid: 22586103
16. S. Etzold *et al.*, Number of growth days and not length of the growth period determines radial stem growth of temperate trees. *Ecol. Lett.* **25**, 427–439 (2022). doi: 10.1111/ele.13933; pmid: 34882952
17. T. Luo *et al.*, Summer solstice marks a seasonal shift in temperature sensitivity of stem growth and nitrogen-use efficiency in cold-limited forests. *Agric. For. Meteorol.* **248**, 469–478 (2018). doi: 10.1016/j.agrformet.2017.10.029
18. C. Dow *et al.*, Warm springs alter timing but not total growth of temperate deciduous trees. *Nature* **608**, 552–557 (2022). doi: 10.1038/s41586-022-05092-3; pmid: 35948636
19. C. Körner *et al.*, Where, why and how? Explaining the low-temperature range limits of temperate tree species. *J. Ecol.* **104**, 1076–1088 (2016). doi: 10.1111/1365-2745.12574

20. Y. S. H. Fu *et al.*, Variation in leaf flushing date influences autumnal senescence and next year's flushing date in two temperate tree species. *Proc. Natl. Acad. Sci. U.S.A.* **111**, 7355–7360 (2014). doi: 10.1073/pnas.1321727111; pmid: 24799708
21. C. M. Zohner, A. Rockinger, S. S. Renner, Increased autumn productivity permits temperate trees to compensate for spring frost damage. *New Phytol.* **221**, 789–795 (2019). doi: 10.1111/nph.15445; pmid: 30240028
22. Y. H. Fu *et al.*, Larger temperature response of autumn leaf senescence than spring leaf-out phenology. *Glob. Change Biol.* **24**, 2159–2168 (2018). doi: 10.1111/gcb.14021; pmid: 29245174
23. C. M. Zohner, S. S. Renner, Ongoing seasonally uneven climate warming leads to earlier autumn growth cessation in deciduous trees. *Oecologia* **189**, 549–561 (2019). doi: 10.1007/s00442-019-04339-7; pmid: 30684009
24. I. Beil, J. Kreyling, C. Meyer, N. Lemcke, A. V. Malyshev, Late to bed, late to rise—Warmer autumn temperatures delay spring phenology by delaying dormancy. *Glob. Change Biol.* **27**, 5806–5817 (2021). doi: 10.1111/gcb.15858; pmid: 34431180
25. M. J. Paul, C. H. Foyer, Sink regulation of photosynthesis. *J. Exp. Bot.* **52**, 1383–1400 (2001). doi: 10.1093/jexbot/52.360.1383; pmid: 11457898
26. Y. Vitasse *et al.*, Impact of microclimatic conditions and resource availability on spring and autumn phenology of temperate tree seedlings. *New Phytol.* **232**, 537–550 (2021). doi: 10.1111/nph.17606; pmid: 34235742
27. W. Buermann *et al.*, Widespread seasonal compensation effects of spring warming on northern plant productivity. *Nature* **562**, 110–114 (2018). doi: 10.1038/s41586-018-0555-7; pmid: 30283105
28. C. Bigler, Y. Vitasse, Premature leaf discoloration of European deciduous trees is caused by drought and heat in late spring and cold spells in early fall. *Agric. For. Meteorol.* **307**, 108492 (2021). doi: 10.1016/j.agrformet.2021.108492
29. P. O. Lim, H. J. Kim, H. G. Nam, Leaf senescence. *Annu. Rev. Plant Biol.* **58**, 115–136 (2007). doi: 10.1146/annurev.arplant.57.032905.105316; pmid: 17177638
30. Y. Fracheboud *et al.*, The control of autumn senescence in European aspen. *Plant Physiol.* **149**, 1982–1991 (2009). doi: 10.1104/pp.108.133249; pmid: 19201914
31. N. Jiang *et al.*, Warming does not delay the start of autumnal leaf coloration but slows its progress rate. *Glob. Ecol. Biogeogr.* **31**, 2297–2313 (2022). doi: 10.1111/geb.13581
32. M. L. Goulden, J. W. Munger, S. M. Fan, B. C. Daube, S. C. Wofsy, Exchange of carbon dioxide by a deciduous forest: Response to interannual climate variability. *Science* **271**, 1576–1578 (1996). doi: 10.1126/science.271.5255.1576
33. C. M. Zohner, S. S. Renner, V. Sebald, T. W. Crowther, How changes in spring and autumn phenology translate into growth-experimental evidence of asymmetric effects. *J. Ecol.* **109**, 2717–2728 (2021). doi: 10.1111/1365-2745.13682
34. M. Friedl, J. Gray, D. Sulla-Menashe, MCD12Q2 MODIS/Terra +Aqua Land Cover Dynamics Yearly L3 Global 500m SIN Grid V006, NASA EOSDIS Land Processes DAAC (2019); https://doi.org/10.5067/MODIS/MCD12Q2.006.
35. B. Templ *et al.*, Pan European Phenological database (PEP725): A single point of access for European data. *Int. J. Biometeorol.* **62**, 1109–1113 (2018). doi: 10.1007/s00484-018-1512-8; pmid: 29455297
36. J. O'Keefe, Phenology of Woody Species at Harvard Forest since 1990, v. 33, Environmental Data Initiative (2021); https://doi.org/10.6073/pasta/91e3b7c2548a0f2e251729eeacbce312.
37. G. Pastorello *et al.*, The FLUXNET2015 dataset and the ONEFlux processing pipeline for eddy covariance data. *Sci. Data* **7**, 225 (2020). doi: 10.1038/s41597-020-0534-3; pmid: 32647314
38. Materials and methods are available as supplementary materials.
39. S. Running, Q. Mu, M. Zhao, MOD17A2H MODIS/Terra Gross Primary Productivity 8-Day L4 Global 500m SIN Grid V006, NASA EOSDIS Land Processes DAAC (2015); https://doi.org/10.5067/MODIS/MOD17A2H.006.
40. Z. Wu *et al.*, Atmospheric brightening counteracts warming-induced delays in autumn phenology of temperate trees in Europe. *Glob. Ecol. Biogeogr.* **30**, 2477–2487 (2021). doi: 10.1111/geb.13404
41. S. Fatichi, S. Leuzinger, C. Körner, Moving beyond photosynthesis: From carbon source to sink-driven vegetation modeling. *New Phytol.* **201**, 1086–1095 (2014). doi: 10.1111/nph.12614; pmid: 24261587
42. F. Pantin, T. Simonneau, B. Muller, Coming of leaf age: Control of growth by hydraulics and metabolics during leaf ontogeny.

New Phytol. **196**, 349–366 (2012). doi: 10.1111/j.1469-8137.2012.04273.x; pmid: 22924516

43. Y. Vitasse *et al*., Elevational adaptation and plasticity in seedling phenology of temperate deciduous tree species. *Oecologia* **171**, 663–678 (2013). doi: 10.1007/s00442-012-2580-9; pmid: 23306445

44. A. J. Elmore, D. M. Nelson, J. M. Craine, Earlier springs are causing reduced nitrogen availability in North American eastern deciduous forests. *Nat. Plants* **2**, 16133 (2016). doi: 10.1038/nplants.2016.133; pmid: 27618399

45. R. E. Mason *et al*., Evidence, causes, and consequences of declining nitrogen availability in terrestrial ecosystems. *Science* **376**, eabh3767 (2022). doi: 10.1126/science.abh3767; pmid: 35420945

46. P. M. Groffman *et al*., Nitrogen oligotrophication in northern hardwood forests. *Biogeochemistry* **141**, 523–539 (2018). doi: 10.1007/s10533-018-0445-y

47. Q. Liu *et al*., Delayed autumn phenology in the Northern Hemisphere is related to change in both climate and spring phenology. *Glob. Change Biol.* **22**, 3702–3711 (2016). doi: 10.1111/gcb.13311; pmid: 27061925

48. G. Liu, X. Chen, Y. Fu, N. Delpierre, Modelling leaf coloration dates over temperate China by considering effects of leafy season climate. *Ecol. Modell.* **394**, 34–43 (2019). doi: 10.1016/j.ecolmodel.2018.12.020

49. X. Lu, T. F. Keenan, No evidence for a negative effect of growing season photosynthesis on leaf senescence timing. *Glob. Change Biol.* **28**, 3083–3093 (2022). doi: 10.1111/gcb.16104; pmid: 35174579

50. L. Marqués *et al*., Acclimation of phenology relieves leaf longevity constraints in deciduous forests. *Nat. Ecol. Evol.* **7**, 198–204 (2023). doi: 10.1038/s41559-022-01946-1; pmid: 36635342

51. C. Wu *et al*., Contrasting responses of autumn-leaf senescence to daytime and night-time warming. *Nat. Clim. Chang.* **8**, 1092–1096 (2018). doi: 10.1038/s41558-018-0346-z

52. X. Zhang, M. Friedl, G. Henebry, VIIRS/NPP Land Cover Dynamics Yearly L3 Global 500m SIN Grid V001, NASA EOSDIS Land Processes DAAC (2020); https://doi.org/10.5067/VIIRS/VNP22Q2.001.

53. M. Rodell *et al*., The Global Land Data Assimilation System. *Bull. Am. Meteorol. Soc.* **85**, 381–394 (2004). doi: 10.1175/BAMS-85-3-381

54. B. Smith *et al*., Implications of incorporating N cycling and N limitations on primary production in an individual-based dynamic vegetation model. *Biogeosciences* **11**, 2027–2054 (2014). doi: 10.5194/bg-11-2027-2014

55. C. Signarbieux *et al*., Asymmetric effects of cooler and warmer winters on beech phenology last beyond spring. *Glob. Change Biol.* **23**, 4569–4580 (2017). doi: 10.1111/gcb.13740; pmid: 28464396

56. C. M. Zohner *et al*., Effect of climate warming on the timing of autumn leaf senescence reverses after the summer solstice, version 1.1, Zenodo (2023); https://doi.org/10.5281/zenodo.7797289.

Effect of climate warming on the timing of autumn leaf senescence reverses after the summer solstice

Constantin M. Zohner, Leila Mirzagholi, Susanne S. Renner, Lidong Mo, Dominic Rebindaine, Raymo Bucher, Daniel Palou, Yann Vitasse, Yongshuo H. Fu, Benjamin D. Stocker, and Thomas W. Crowther

Editor's summary

Global warming is changing the timing of photosynthesis, with leaves emerging earlier in spring in the temperate and boreal zones. A longer growing season could mean greater carbon sequestration in forests, but the timing of leaves falling in autumn depends on multiple cues, making it difficult to predict. Zohner *et al.* investigated how leaf senescence relates to day length, temperature, and early-season photosynthesis across northern forests using remote sensing, ground observations, and experimental data. They found that warming had opposing effects on senescence dates depending on when it occurred: Warmer springs with higher photosynthesis correlated with earlier senescence, wheras warmer temperatures in autumn delayed senescence. Incorporating this shift in knowledge may improve predictions of vegetation response to climate change. —BEL

View the article online
https://www.science.org/doi/10.1126/science.adf5098
Permissions
https://www.science.org/help/reprints-and-permissions

Use of this article is subject to the Terms of service